The chemistry of the superheavy elements. II. The stability of high oxidation states in group 11 elements: Relativistic coupled cluster calculations for the di-, tetra- and hexafluoro metallates of Cu, Ag, Au, and element 111

Michael Seth, Fiona Cooke, and Peter Schwerdtfeger[a)]
Department of Chemistry, The University of Auckland, Private Bag 92019, Auckland, New Zealand

Jean-Louis Heully
Laboratoire de Physique Quantique, URA 505 du CNRS, Université Paul Sabatier, 118, route de Narbonne, 31062 Toulouse Cedex, France

Michel Pelissier
Chimie 4, Université de Poitiers, 40, avenue du Recteur Pineau, F-86022 Poitiers, France

(Received 14 April 1998; accepted 5 June 1998)

The stability of the high oxidation states +3 and +5 in Group 11 fluorides is studied by relativistic Møller–Plesset (MP) and coupled cluster methods. Higher metal oxidation states are stabilized by relativistic effects. As a result, the hexafluoro complex of the Group 11 element with nuclear charge 111 and oxidation state +5 is the most stable compared to the other congeners. The results also suggest that AgF_6^- is thermodynamically stable and, therefore, it might be feasable to synthesize this compound. For the copper fluorides we observe very large oscillations in the Møller–Plesset series up to the fourth order. Nonrelativistic calculations lead to the expected trend in the metal–fluorine bond distances for the MF_2^- compounds, $CuF_2^- < AgF_2^- < AuF_2^- < (111)F_2^-$. However, relativistic effects change this trend to $CuF_2^- < AuF_2^- < (111)F_2^- < AgF_2^-$. Vibrational frequencies are predicted for all compounds. Where experimental data are available, they generally agree very well with our calculated results. © *1998 American Institute of Physics.* [S0021-9606(98)30334-7]

INTRODUCTION

It is well known that the Group 11 elements show an unusual trend in the stability of the oxidation states.[1] The most common oxidation states are +2 for copper, +1 for silver, +1 and +3 for gold. For the next congener, a transactinide with nuclear charge $Z=111$ (named element 111 in the following), atomic calculations by Fricke suggest that the most stable oxidation state is +3, similar to that of gold.[2] Element 111 was discovered recently by the Heavy Ion Research Laboratory (GSI) in Darmstadt.[3] The chemistry of short lived isotopes with half times in the second range (atom-at-a-time chemistry) can give indirect evidence of the stability of high oxidation states.[4] However, the isotope $^{272}111$ has an estimated half life of only 2 ms and the synthesis of more neutron-rich isotopes requires a radioactive beam facility which is not available yet.[5] Hence, theoretical methods seem at present the only way to gain insight into physical and chemical properties of element 111. On the other hand, theoretical studies on copper and silver compounds in high oxidation states (+3 or +5) are very rare.[6]

In two recent papers it was shown that the high oxidation states +3 and +5 in gold are significantly stabilized by relativistic effects.[7,8] It is now well established that compounds containing Group 11 elements exhibit large relativistic effects (the Group 11 maximum of relativistic effects)[9] causing anomalies in chemical properties of gold.[10–13] Further down the group, element 111 shows extremely large relativistic effects[14,15] which even cause a change in the ground electronic state configuration from $d^{10}s^1$ to d^9s^2.[14] Moreover, the diatomic compound (111)H has a bond distance similar to that of CuH due to the large relativistic bond contraction.[15] This contraction is especially large for electropositive ligands,[12] but much smaller in compounds of gold in high oxidation states.[7,8] In this article we examine all group 11 elements (Cu, Ag, Au, and element 111) in the oxidation states +1, +3, and +5. Since the fluorine ligand offers the best chance to isolate copper or silver compounds with the metal being in the oxidation state +5, we will concentrate the following fluorine species: MF_2^-, MF_4^-, and MF_6^- (M=Cu, Ag, Au, and element 111). CuF_4^-, AuF_4^-, and AuF_6^- are characterized by x-ray crystallography,[16–21] but beside the solid-state structure and vibrational frequencies for the gold species there is not much known about these compounds.

COMPUTATIONAL DETAILS

Small core 19 valence-electron energy consistent scalar relativistic and nonrelativistic pseudopotentials were applied for the metal atoms M=Cu, Ag, Au, and element 111. The semilocal pseudopotential for core λ used has the following functional form:

a)Author to whom correspondence should be addressed. Electronic mail: schwerd@ccu1.auckland.ac.nz

TABLE I. Gaussian type basis sets used in the molecular calculations.[a]

Atom	Size	Method	Primitives	Contracted	*f*-exponents
Cu	*S*	RPP	$9s7p6d2f$	$6s5p5d2f$	1.3375, 0.4
	L	RPP	$9s7p6d2f$	$7s6p5d2f$	1.3375, 0.4
	L	NRPP	$10s7p6d2f$	$9s6p5d2f$	1.3375, 0.4
	L	NRAE	$20s15p10d6f$	$7s6p4d3f$	24.705, 9.88121, 3.9528, 1.5811, 0.6325, 0.253
	L	DKAE	$20s15p10d3f$	gc $10s9p7d3f$	3.9528, 1.5811, 0.6325
Ag	*S*	RPP	$9s7p6d2f$	$6s5p5d2f$	1.3, 0.5
	L	RPP	$9s7p6d2f$	$7s6p5d2f$	1.3, 0.5
	L	NRPP	$10s7p6d2f$	$9s6p5d2f$	1.3, 0.5
Au	*S*	RPP	$9s7p6d2f$	$6s5p5d2f$	1.1447, 0.4
	L	RPP	$9s7p6d2f$	$7s6p5d2f$	1.1447, 0.4
	L	NRPP	$10s7p6d2f$	$9s6p5d2f$	1.1447, 0.4
111	*S*	RPP	$9s7p6d2f$	$6s5p5d2f$	2.05, 0.88
	L	RPP	$9s7p6d2f$	$7s6p5d2f$	2.05, 0.88
	L	NRPP	$10s7p6d2f$	$9s6p5d2f$	1.80, 0.89
F	*S*	NRAE	$9s4p1d$	$3s2p1d$	
	L	NRAE	$11s6p2d$	$5s4p2d$	

[a]*S* and *L* denotes the small and the large basis set, respectively. RPP: Scalar (ARPP) or spin–orbit coupled relativistic pseudopotential. NRPP: Nonrelativistic pseudopotential. AE: All-electron. DK: scalar Douglas–Kroll Hamiltonian. The large fluorine basis set is based on Dunning's aug-cc-PVTZ basis set, the small one is Dunning's cc-PVDZ basis set. gc denotes that a general contraction scheme was used.

$$V_{\lambda}^{PP}(r_{i\lambda}) = -\frac{Q_{\lambda}}{r_{i\lambda}} + \sum_{l} P_{l\lambda} \sum_{k} f_{kl\lambda}(r_{i\lambda}). \tag{1}$$

Q_{λ} is the charge of core λ ($Q_{\mathrm{M}}=19$ for all metals), $f_{1\lambda}$ is a linear combination of Gaussian functions containing adjustable parameters (usually two Gaussian functions per angular momentum are used in the Stuttgart pseudopotential scheme, i.e., $k=2$), and $P_{1\lambda}$ is the projection operator onto the Hilbert subspace with angular symmetry *l*. Spin–orbit coupling was included for Au and element 111 through the use of spin–orbit coupled pseudopotentials. The parameters for the pseudopotentials used can be found in our first paper in this series of superheavy elements[25] and in Refs. 12, 22–24. The geometries of all molecules were optimised at the MP2 level using the Fletcher–Powell method. The MF_2^-, MF_4^-, and MF_6^- molecules were restricted to have $D_{\infty h}$, D_{4h}, and O_h symmetry, respectively.

The valence basis sets used are summarized in Table I. The relativistic and nonrelativistic basis set for element 111 is that given in Ref. 25 but with the most diffuse *s*, *p*, and *d* functions removed. Only two uncontracted *f* functions were used for all metals. In order to have matching basis sets for Cu, Ag, and Au new basis sets were optimized and contracted. The new basis sets were energy optimized using the ATMSCF program[26] and in all cases gave Hartree–Fock (HF) energies lower than the published ones. The exponents and contraction coefficients for all elements are shown in Table II. The *f*-exponents were taken from Refs. 8, 25, and 27. The nonrelativistic basis sets contain one more diffuse *s*-function compared to the relativistic ones because the nonrelativistic valence *s*-orbitals are more diffuse. The fluorine basis set used is based upon the augmented correlation consistent valence triple-zeta polarization basis set (aug-cc-PVTZ) of Dunning.[28] The two fluorine *f* functions were removed and the contracted $3d$ set was replaced with the $2d$ set from the double-zeta basis set.

We carried out single-point coupled cluster calculations [CCSD and CCSD(T), which includes the triple corrections perturbatively] at the optimized MP2 geometry in order to establish the stability of the high oxidation state by studying the decomposition reaction (ΔU is the decomposition energy)

$$MF_n^- \rightarrow MF_{n-2}^- + F_2 + \Delta U. \tag{2}$$

The geometry optimizations were carried out using GAUSSIAN94[29] followed by a frequency calculation to verify that a local minimum was obtained. A modified version of the program package MOLCAS3[30] was used for the subsequent correlation treatment. This program was altered to include routines for the one-electron integrals required for the semilocal pseudopotentials.[31] For this purpose we transformed the semilocal part of the pseudopotential to a linear combination of nonlocal projection operators consisting of Cartesian Gaussian functions g_m

$$W_{\lambda}^{PP}(r_{i\lambda}) \cong \sum_{m} |g_m(r_{i\lambda})\rangle\langle g_m(r_{i\lambda})|. \tag{3}$$

The method has been developed by Pelissier *et al.*[31] and has the advantage that only overlap integrals over cartesian Gaussian functions are needed. We used an even tempered sequence of exponents resulting usually in 35–38 Gaussians per symmetry. For all the Group 11 elements the difference in the total electronic energy between the two different pseudopotential representations (1) and (3) is less than 10^{-5} a.u. for the neutral atoms. The coupled cluster program TITAN by Lee *et al.* was interfaced with MOLCAS3.[32]

It was not possible to treat the MF_6^- molecules at the CCSD level using the large basis sets described above. We, therefore, had to reduce the basis set slightly which we will denote as the small basis set *S* in the following. For the metal atoms we used the same number of primitives as for the large

TABLE II. Exponents and contraction coefficients for the valence basis sets of Cu, Ag, and Au.[a]

Nonrelativistic Cu	
s	(25.254 925, 15.583 150, 7.720 108 3; 0.137 495 64, −0.266 535 12, −0.335 371 81)
	3.688 33 63, 1.729 78 14, 0.774 237 79, 0.173 075 10, 0.082 246 924, 0.033 099 100, 0.011 033 033
p	(15.580 203, 5.129 400 9; 0.094 283 526, −0.233 201 58)
	2.479 912 3, 1.152 727 3, 0.531 400 82, 0.101 978 36, 0.028 299 351
d	(46.031 604, 14.245 856; 0.030 024 914, 0.145 700 26)
	5.148 200 2, 1.915 977 7, 0.681 052 68, 0.215 403 72
Relativistic Cu	
s	(26.533 189, 15.349 632, 7.718 628 4; 0.120 554 04, −0.266 337 11, −0.315 720 45)
	3.690 701 3, 1.738 567 4, 0.784 187 83, 0.184 931 01, 0.085 071 170, 0.034 114 076
p	(15.793 101, 5.129 400 9; −0.091 745 948, 0.238 219 12)
	2.479 912 3, 1.152 727 3, 0.531 400 82, 0.101 978 36, 0.028 299 351
d	(46.031 604, 14.245 856; 0.030 650 159, 0.145 308 99)
	5.148 200 2, 1.915 977 7, 0.681 207 43, 0.215 403 72
Nonrelativistic Ag	
s	(15.185 671, 14.270 973, 8.348 985 2; −1.156 729 8, 1.497 398 6, −0.391 018 04)
	4.830 954 1, 1.490 409 8, 0.706 972 82, 0.296 967 10, 0.091 324 001, 0.033 441 248, 0.011 147 083
p	(12.103 285, 11.178 389; −0.152 156 12, 0.091 228 187)
	7.718 778 1, 1.926 040 8, 0.894 521 99, 0.396 530 24, 0.126 335 73
d	(7.469 405 8, 3.058 180 0; 0.023 234 797, −0.208 501 99)
	1.381 155 8, 0.593 209 67, 0.247 132 58, 0.098 996 873
Relativistic Ag	
s	(18.818 321, 14.298 365, 7.347 068; −0.129 730 30, 0.376 520 24, −0.425 612 60)
	4.957 451, 1.518 658, 0.702 863, 0.250 614, 0.095 901, 0.035 614
p	(12.534 842, 10.786 385; −0.085 409 092, −0.010 617 090)
	8.162 106, 1.938 228, 0.886 148, 0.385 358, 0.115 329
d	(7.314 669, 3.081 480; 0.021 424 896, −0.205 198 63)
	1.377 450, 0.587 87, 0.243 210, 0.096 862
Nonrelativistic Au	
s	(12.264 729, 10.857 927, 8.695 161 3; −0.175 523 95, 0.322 907 02, −0.141 675 94)
	4.059 165 8, 1.340 619 1, 0.672 034 09, 0.301 839 37, 0.091 101 522, 0.033 559 602, 0.011 186 534
p	(18.969 765, 12.862 245; 0.183 376 72, −0.824 510 06)
	5.593 511 2, 1.659 470 4, 0.863 843 06, 0.416 150 32, 0.158 965 23
d	(4.129 816 5, 3.306 167 7; 0.274 719 66, −0.315 266 57)
	1.249 036 5, 0.543 140 59, 0.228 734 45, 0.092 288 501
Relativistic Au	
s	(18.522 519, 12.532 822, 7.426 954; −0.173 435 22, 0.655 662 24, −0.698 239 92)
	4.446 247, 1.475 416, 0.693 121, 0.238 482, 0.103 156, 0.041 208
p	(18.687 648, 14.425 298; 0.038 936 284, −0.105 629 160)
	6.161 932, 1.735 913, 0.855 223, 0.393 101, 0.137 244
d	(4.315 372, 3.260 757; 0.204 868 38, −0.244 587 23)
	1.258 506, 0.542 233, 0.223 880, 0.088 536

[a]Contraction coefficients are set in brackets behind the exponents. For the *f*-exponents see Table I. For these basis sets we obtain the total valence electronic energies (all values in a.u.): Cu −195.636 511 04 (NR), Cu −196.221 688 82 (R), Ag −146.117 845 64 (NR), Ag −144.996 224 85 (R), Au −130.836 108 37 (NR), Au −130.970 399 28 (R). NR and R denotes the nonrelativistic and scalar relativistic pseudopotential approximation, respectively.

basis set *L*, but more heavily contracted, see Table I. The fluorine basis set is the correlation consistent polarization valence double-zeta set of Dunning.[28]

The copper fluorides showed unexpected changes in the electron correlation contribution to the total electronic energy compared to the other Group 11 metals. An analysis showed a very large oscillatory behavior in the MP*n* series [$n=1$ (HF), 2, 3, and 4]. A critical account on the use of the MP series for transition metal atoms has been given by Raghavachari and Trucks who pointed that for the *d*-elements the MP series does not converge very well.[33] Furthermore, it is well known that MP convergence for the fluorides is usually less good compared to the hydrides.[34] However, CuF_6^- showed an extremely large change in the electron correlation contribution to the decomposition energy (2) of more than 1000 kJ/mol (!) at the MP2 level, much larger than the changes reported by Ragavachari and Trucks.[33] In order to exclude the possibility that this is caused by the pseudopotential approximation we carried out both nonrelativistic and scalar relativistic Douglas–Kroll calculations for CuF_2^-, CuF_4^-, and CuF_6^-. The all-electron calculations were carried out using the large $20s15p10d$ exponent set given by Partridge.[35] The primitives were generally contracted to $10s9p7d$ and three of the *f*-functions given by Bauschlicher were added,[36] see Table I. For the nonrelativistic all-electron calculation we used the Bauschlicher atomic natural orbital (ANO) contraction scheme.[36] The *g*-functions from Ref. 36 were omitted but the six *f* primitives contracted to a $3f$ set were included. The fluorine basis set used in the all-electron calculations was the same as in basis *L*. The matrix elements over the scalar version of the second-order Douglas–Kroll Hamiltonian[37] were evaluated using the routines written by Heß.[38]

The frequency analyses were carried out at the MP2 level using the large basis but with the *f* functions removed. All geometries were of course re-optimized at the MP2 level with this smaller basis set. The MP2 frequency analysis gave, however, unrealistic results for CuF_6^- indicating that the MP2 hypersurface is ill-defined. A similar behavior was found for MnO_4^- where the stretching of one of the Mn–O bonds leads to a double-minimum potential at the MP2 level.[39] Hence, for CuF_6^- we list HF rather than MP2 frequencies. However, to obtain a measure of the accuracy of our predictions for all compounds, we decided to perform density functional calculations. It was pointed out by Baerends *et al.* that in such cases density functional theory describes the metal-ligand bonding significantly better.[40] We, therefore, used Becke's hybrid method using a three parameter functional together with the Lee–Yang–Parr nonlocal correlation functional (denoted as B3LYP).[41,42]

A modified version of the COLUMBUS program which utilises double-group symmetry at the configuration interaction (CI) step was used for the spin–orbit coupled calculations.[43] Due to program limitations only very small basis sets could be used in the spin–orbit coupled CI calculations.[43] For the metal atoms (Au and element 111) a $9s8p6d$ set contracted to $5s3p4d$ set was used and for F the correlation consistent valence double-zeta polarized (cc-PVDZ) basis set of Dunning was used as described

TABLE III. Optimized fluorine–metal bond distances.[a]

	Cu		Ag		Au		111	
Molecule	NR	R	NR	R	NR	R	NR	R
MF_2^-	1.780	1.766	2.060	1.998	2.134	1.959	2.328	1.967
MF_4^-	1.737	1.727	1.924	1.898	1.988	1.919	2.116	1.953
MF_6^-	1.885	1.872	1.950	1.920	1.984	1.917	2.092	1.951

[a]Bond distances r_e are in Å. The geometries are obtained from MP2 geometry optimizations using the large basis set.

above, but with the *d* function deleted. A diffuse *p*-function with exponent 0.03 was added to the metal atoms to describe the radial splitting between the $np_{1/2}$ and $np_{3/2}$ virtual orbitals (in the $6d^9 7s^1 7p^1$ configuration of neutral element 111 the *r*-expectation values are $\langle r\rangle_{7p_{1/2}} = 3.5$ a.u. and $\langle r\rangle_{7p_{3/2}} = 5.0$ a.u.). The molecular orbitals from a scalar relativistic pseudopotential calculation were used in a very limited CI procedure with single and double substitutions (CISD restricted to two open shells with 42, 32, and 22 active electrons for MF_2^-, MF_4^-, and MF_6^-, respectively). All molecular orbitals (MO) with an orbital energy greater than 1 a.u. were deleted. The spin–orbit coupled pseudopotential parameters are given in Ref. 25 for element 111 and Ref. 23 for Au. The spin–orbit correction was determined by taking the difference between the spin–orbit CI energy and the energy obtained from an equivalent calculation in which the spin–orbit potentials are set to zero. This correction was then added to an energy derived from a more complete scalar relativistic electron correlation treatment.

To test the quality of the MP2 geometries the structures for $(111)F_4^-$ and $(111)F_2^-$ molecules were determined at the CCSD(T) level by a polynomial fit to five or six calculated energies. The CCSD(T) bond lengths were only 0.008 and 0.012 Å longer than the MP2 values for $(111)F_4^-$ and $(111)F_2^-$, respectively. The influence of spin–orbit coupling on the geometry was also investigated for these two molecules. Spin–orbit coupling decreases the bond length 0.001 Å for $(111)F_4^-$ and 0.007 Å for $(111)F_2^-$. The optimized MP2 bond distance of F_2 is 1.413 Å in good agreement with the experimental result (1.412 Å).[44]

RESULTS AND DISCUSSION

The calculated nonrelativistic and relativistic MP2 bond distances are shown in Table III. Fleischer and Hoppe report 1.73 Å for the Cu–F bond distance from a powder diffraction study of $CsCuF_4$[16] in excellent agreement with our calculated value of 1.727 Å. A CCSD(T) optimization at the all-electron Douglas–Kroll (DK) level leads to a slightly larger bond distance of 1.753 Å. $KAgF_4$ has been synthesized by Hoppe[17] but we are not aware of any crystal structure determination. The Au–F bond distance has been measured by Edwards in $KAuF_4$ (1.95 Å)[20] and is in reasonable agreement with our calculated value of 1.919 Å. The difference between the two values is due to solid-state effects and the level of approximation used in our calculations. All compounds are diamagnetic in the oxidation state +3 and we, therefore, considered only the singlet electronic state. Bartlett and coworkers synthesized $[Xe_2F_{11}^+][AuF_6^-]$[19] and both the crystal structure and Raman spectrum has been determined.[21] The measured Au–F bond distance ranges between 1.85 and 1.90 Å (due to the different solid-state environments) and is in reasonable agreement with our calculated MP2 value of 1.917 Å.

The relativistic effects in the equilibrium bond distances are depicted in Fig. 1. It is evident that the largest relativistic effects are obtained in the low oxidation state, +1. Relativistic bond contractions in the fluorides of the higher oxidation states, +3 and +5, are of similar size but significantly smaller compared to the MF_2^- species. As pointed out before,[8] this is directly related to the occupation of the valence *ns* orbital, which decreases with increasing oxidation state, and the participation of the valence $(n-1)d$ orbital, which increases with increasing oxidation state. This is clearly seen from the Mulliken orbital *ns* and $(n-1)d$ populations listed in Table IV.

Figure 1 also shows what is expected, that relativistic bond contractions increase from Cu to 111. As a consequence we obtain the following sequence in the metal–fluorine (M–F) bond distances: $CuF_2^- < AuF_2^- < (111)F_2^- < AgF_2^-$. The nonrelativistic bond distances show the trend we usually expect, $CuF_2^- < AgF_2^- < AuF_2^- < (111)F_2^-$. Furthermore, the different size of relativistic effects leads to the interesting result that the (111)-F bond distances are very similar for the element in all three oxidation states. Another interesting point concerns the M–F bond distance for the metal M in the oxidation state +5. For Au and element 111 the M–F bond distance in MF_6^-

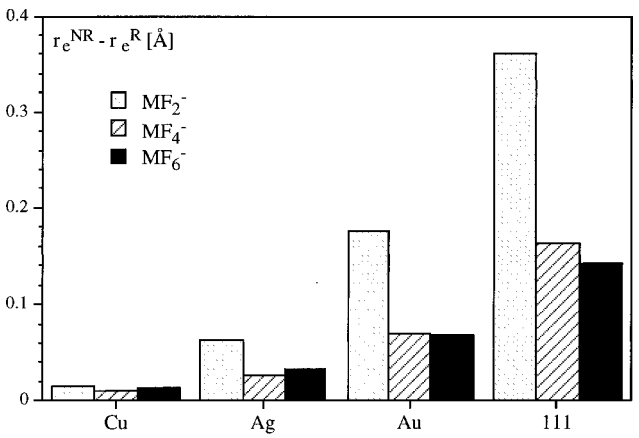

FIG. 1. A comparison of relativistic bond contractions for Group 11 fluorides at the MP2 level.

TABLE IV. Mulliken population analysis for the metal M (M=Cu, Ag, Au, and 111).[a]

		Cu		Ag		Au		111	
Molecule	Property	NR	R	NR	R	NR	R	NR	R
MF_2^-	q	0.61	0.59	0.74	0.71	0.82	0.62	0.81	0.52
	$(n-1)d_\sigma$	1.61	1.59	1.81	1.75	1.65	1.48	1.89	0.99
	$(n-1)d_\pi$	4.02	4.02	4.02	4.01	4.00	4.00	4.02	3.98
	$(n-1)d_\delta$	4.00	4.00	4.00	4.00	4.00	4.00	4.00	4.00
	ns	0.67	0.70	0.35	0.45	0.48	0.83	0.22	1.49
	np_σ	0.01	0.02	0.03	0.03	−0.01	0.01	0.03	−0.06
	np_π	0.06	0.08	0.05	0.05	0.05	0.05	0.03	0.06
MF_4^-	q	1.56	1.56	1.81	1.78	1.87	1.88	1.98	1.95
	$(n-1)d$	8.99	8.99	8.99	8.95	8.91	8.69	8.96	8.17
	ns	0.27	0.28	0.11	0.16	0.15	0.33	0.01	0.80
	np	0.17	0.18	0.09	0.11	0.06	0.09	0.05	0.03
MF_6^-	q	2.47	2.37	2.46	2.57	2.67	2.83	2.89	3.17
	$(n-1)d$	8.74	8.69	8.48	8.35	8.27	7.98	8.22	7.45
	ns	−0.29	−0.15	−0.03	0.00	−0.02	0.08	−0.16	0.25
	np	0.09	0.09	0.08	0.08	0.08	0.11	0.05	0.14

[a]The population analyses were carried out at the B3LYP level. q represents the total metal charge.

is slightly shorter than the one in MF_4^-. This is what we usually expect when going to the higher oxidation state. However, for AgF_6^- and CuF_6^- the M–F bond distance is significantly larger compared to the ones in MF_4^-. This indicates that both AgF_6^- and CuF_6^- may not be very stable thermodynamically.

The Raman frequencies for both AuF_4^- and AuF_6^- have been reported by Bartlett and co-workers. They are compared with our calculated MP2 and B3LYP frequencies in Table V. Considering that our results are gas-phase calculations of the free anion and the frequencies do not contain anharmonicity effects, they are in excellent agreement with the results by Bartlett *et al.* Our calculated frequencies and infrared intensities may, therefore, help in the frequency assignment of the yet unknown remaining Group 11 fluorides. The frequencies show that all structures represent local minima on the potential-energy surface for the free anion. Hence all species are (kinetically) stable compounds.

Concerning the thermodynamic stability of these compounds we calculated the reaction energy for the decomposition of the fluoro complexes in the higher oxidation states, Eq. (2). The results are presented in Tables VI and VII. The relativistic coupled cluster and the density functional results show that the higher oxidation states are preferred by the heavier elements. Element 111 shows the highest stability in the oxidation states +3 and +5. Relativistic effects clearly

TABLE V. Vibrational frequencies and IR intensities for the group 11 metal fluorides.[a]

Irreducible representation	Cu		Ag		Au		
	RMP2	B3LYP	RMP2	B3LYP	RMP2	B3LYP	exp.
$MF_6^-(O_h)$							
T_{1u}	783 (217)	642 (84)	595 (33)	617 (120)	623 (117)	609 (140)	
A_{1g}	662 (0)	538 (0)	453 (0)	525 (0)	561 (0)	566 (0)	595
E_g	604 (0)	484 (0)	463 (0)	516 (0)	570 (0)	563 (0)	530
T_{1u}	371 (7)	318 (0.08)	233 (1)	275 (1)	244 (2)	263 (4)	
T_{2g}	342 (0)	269 (0)	191 (0)	220 (0)	217 (0)	205 (0)	224
T_{2u}	267 (0)	217 (0)	186 (0)	212 (0)	200 (0)	221 (0)	
$MF_4^-(D_{4h})$							
E_u	694 (236)	670 (159)	607 (201)	592 (165)	600 (194)	579 (174)	
A_{1g}	586 (0)	566 (0)	524 (0)	517 (0)	586 (0)	554 (0)	588
B_{2g}	545 (0)	508 (0)	518 (0)	487 (0)	581 (0)	534 (0)	561
B_{1g}	314 (0)	315 (0)	231 (0)	247 (0)	221 (0)	221 (0)	230
A_{2u}	290 (35)	289 (38)	215 (33)	237 (33)	205 (23)	222 (23)	
E_u	289 (4)	229 (0.3)	229 (∼0)	260 (1)	235 (2)	249 (3)	
B_{1u}	139 (0)	137	137 (0)	149 (0)	164 (0)	172 (0)	
$MF_2^-(D_{\infty h})$							
Σ_u	622 (140)	602 (138)	471 (151)	480 (151)	529 (176)	512 (174)	
Σ_g	520 (0)	487 (0)	388 (0)	400 (0)	509 (0)	477 (0)	
Π_u	177 (8)	196 (13)	122 (31)	168 (26)	160 (12)	184 (13)	

[a]Harmonic vibrational frequencies in cm^{-1}, infrared intensities in 10^3 m mol^{-1} are set in parentheses. Experimental Raman values by Leary and Bartlett (Ref. 19). In all calculations the metal *f*-functions were omitted and the structures reoptimized. The (x,y) axes of the coordinate system are chosen to bisect the MF_2 angles for MF_4^-.

TABLE VI. Decomposition energies ΔU for the group 11 metal fluorides.[a]

Reaction	Method	Cu	Ag	Au	111
$MF_6^- \rightarrow$	HF	−688.6	−238.4	34.5	264.1
$MF_4^- + F_2$		−729.3	−266.6	16.7	262.7
	MP2	407.1	166.7	227.0	295.1
		396.4	148.0	214.6	304.2
	MP3	−471.4	−36.3	130.8	267.1
	MP4(SDQ)	18.2	−2.2	161.8	279.2
	MP4(SDTQ)	470.8	⋯	⋯	⋯
	CCSD	−241.9	−27.9	134.3	265.6
	CCSD(T)	−91.9	38.1	164.5	273.0
	B3LYP	−68.3	80.8	199.0	284.9
$MF_4^- \rightarrow$	HF	475.0	262.1	407.2	456.6
$MF_2^- + F_2$		462.3	240.5	399.3	458.6
	MP2	178.5	323.5	379.2	417.9
		159.4	297.7	384.6	465.6
	MP3	438.8	292.7	376.0	413.0
	MP4(SDQ)	223.4	312.5	386.3	419.5
	MP4(SDTQ)	179.9	⋯	⋯	⋯
	CCSD	385.7	302.6	379.2	413.0
		370.4	281.1	384.3	452.8
	CCSD(T)	393.8	321.6	381.4	410.5
		383.7	303.0	389.9	455.9
	B3LYP	420.9	357.5	406.6	411.8

[a]All values are in kJ/mol. The calculations are all performed at the scalar relativistic MP2 optimized geometry using the large basis set. The calculations using the larger basis set are given below the one of the smaller basis in italics.

stabilize the high oxidation states. The results indicate that (as far as the fluorides are concerned) element 111 is similar to gold with a more pronounced tendency to the higher oxidation states. Similar trends have recently be found for the Group 12 fluorides of Hg and element 112.[25]

Both CuF_6^- and AgF_6^- are unknown compounds. It came as a surprise when MP2 calculations revealed the CuF_6^- is a stable compound, Fig. 2. However, there is a very large difference between the decomposition energy calculated at the HF and the MP2 level, more than 1100 kJ mol^{-1}. In order to check if this is a defect of the pseudopotential approximation occurring for the oxidation state of copper, we carried out computer time intensive all-electron Hartree–Fock (HF) and (relativistic) Douglas–Kroll (DK) calculations as described in the computational section. At the all-electron level we obtain for the $MF_6^- \rightarrow MF_4^- + F_2$ reaction $\Delta U = 404.7$ kJ mol^{-1} at the nonrelativistic MP2 (NRMP2) level and 376.4 kJ mol^{-1} at the Douglas–Kroll MP2 (DKMP2) level. This compares very well with the pseudopotential results (403.3 kJ mol^{-1} at the NRMP2 level and 396.4 kJ mol^{-1} at the relativistic MP2 level) considering that different basis sets were used. For the reaction $MF_4^- \rightarrow MF_2^- + F_2$ we obtain a similar good agreement for the ΔU values, 131.8 kJ mol^{-1} at the NRMP2 level and 143.9 kJ mol^{-1} at the DKMP2 level compared to the pseudopotential results, 138.9 kJ mol^{-1} at the NRMP2 level and 159.4 kJ mol^{-1} at the

TABLE VII. Comparison between nonrelativistic and relativistic decomposition energies ΔU for the group 11 metal fluorides.[a]

		Cu		Ag		Au		111	
Reaction	Method	NR	R	NR	R	NR	R	NR	R
$MF_6^- \rightarrow$	HF	−755.4	−729.3	−346.9	−266.6	−188.8	16.7	−158.9	262.7
$MF_4^- + F_2$	Δ_RHF		26.1		80.3		205.5		421.6
	MP2	403.3	396.4	128.1	148.0	139.5	214.6	133.8	304.2
	Δ_RMP2		−6.9		−19.9		75.1		170.4
$MF_4^- \rightarrow$	HF	411.8	462.3	135.5	240.5	177.8	399.3	89.2	458.6
$MF_2^- + F_2$	Δ_RHF		50.5		105.0		221.5		369.4
	MP2	138.9	159.4	248.7	297.7	281.8	384.6	272.4	465.6
	Δ_RMP2		20.5		49.0		102.8		193.2
	CCSD	294.2	370.4	211.9	281.1	243.1	384.3	235.2	452.8
	Δ_RCCSD		76.2		69.2		141.2		217.6
	CCSD(T)	355.1	383.7	243.4	303.0	267.7	389.9	205.7	455.9
	Δ_RCCSD(T)		28.6		58.6		122.2		250.2

[a]All values are in kJ/mol. The calculations are all performed using the large basis set at the MP2 optimized geometry.

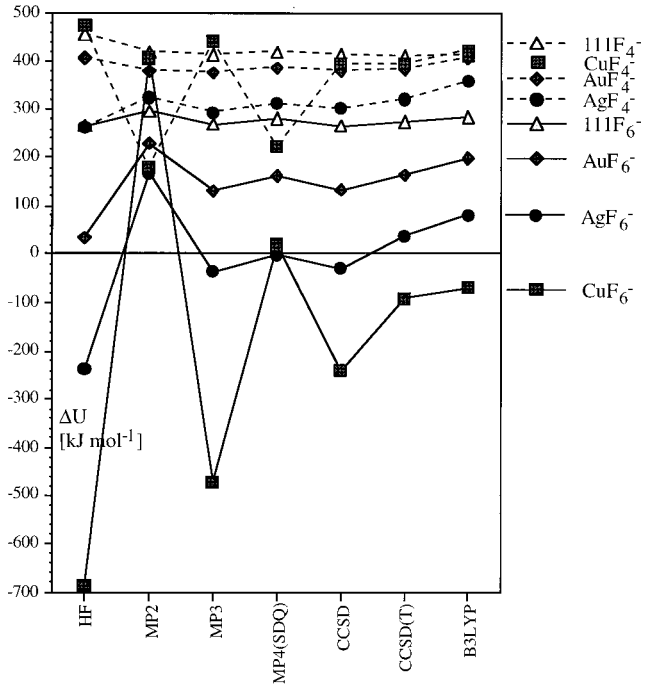

FIG. 2. Decomposition energies ΔU at various levels of theory. Oxidation state +5: $MF_6^- \rightarrow MF_4^- + F_2$. Oxidation state +3: $MF_4^- \rightarrow MF_2^- + F_2$ (M=Cu, Ag, Au, element 111).

relativistic MP2 level. For this reaction we have been able to calculate all-electron coupled-cluster values. At the CCSD(T) level we have $\Delta U = 362.8$ kJ mol^{-1} at the NRMP2 level and 380.7 kJ mol^{-1} at the DKMP2 level. This is again in good agreement with our pseudopotential results giving confidence in the pseudopotential approximation.

Raghavachari and and Trucks[33] pointed out that for the first transition element series the MP series converges badly (if at all). The convergence in particularly bad for the late transition metals. For example, the difference between MP2 and MP3 is about 270 kJ mol^{-1} for the d^9s^2 to $d^{10}s^1$ excitation in neutral copper. They also pointed out that coupled cluster performs reasonably well.[33] Buijse and Baerends analyzed the failure of Hartree–Fock (HF) to account for nondynamical correlation in metal ligand bonding in MnO_4^-.[40] Their conclusion was that because the transition metal $3s/3p$ orbitals are spacially close to the $3d$ orbitals, Pauli repulsion between the metal $3s3p$ and ligand $2p$ orbitals prevents the ligands from getting close to the metal resulting in a small overlap between the metal $3d$ and ligand $2p$ orbitals. In MnO_4^- HF tends to localize the orbitals resulting in a loss of covalent character of the metal–ligand bonding. This can only be corrected through a multiconfiguration (MC) treatment. For CuF_6^- all fluorine lone pairs and the metal *d*-electrons would have to be considered in the MC treatment which is computationally too demanding. For the late second, third, and fourth row transition compounds, the *d*-orbitals are more diffuse and more separated compared to the *sp* orbitals in the same shell. For Au and element 111 this is partly due to the relativistic *d*-expansion. Moreover, the bond distance of the Group 11 hexafluoro complexes are very similar at the relativistic level. This could be because of a reduced Pauli repulsion from the *sp*-core if we accept the interpretation of Buijse and Baerends. Thus the overlap between the metal *d* and the fluorine $2p$ orbitals should increase with going to the heavier elements. Figure 2 shows that while CuF_6^- (and CuF_4^-) shows very large oscillations in the MP*n* series (the largest oscillations at an equilibrium geometry reported so far), this is less the case for AgF_6^- and almost gone for AuF_6^-. Baerends also argued that density functionals do not suffer from this classical HF error.[40] As Fig. 2 shows the B3LYP calculations are closest to the CCSD(T) results.

Analyzing the orbitals of the MF_6^- in O_h symmetry in detail we cannot see a localization of the fluorine *p*- and metal *d*-orbitals. There is a low lying t_{2g}-orbital which is mainly metal-*d*. However, the σ-bonding e_g-orbital is a mixture between fluorine-*p* and metal-*d* with only a slight increase in overlap when going from Cu to element 111. The only significant changes in the MO picture between the different elements we see is that the a_{1g} orbital is lower in energy for the heavier metal (due to the relativistic valence *s*-contraction), and the orbitals representing the fluorine lone pairs are more split in the ligand field for the heavier elements. Moreover, the *sp*-core orbitals contract when going to the late transition metals because of the increasing nuclear charge, thus the Pauli repulsion is reduced. However, we do notice a significant increase in the highest occupied molecular orbital–lowest unoccupied molecular orbital HOMO–LUMO) gap from 0.366 a.u. for Cu to 0.413 a.u. for Ag, to 0.460 a.u. for Au and to 0.554 a.u. for element 111. It is well known that the MP series converges badly for small HOMO–LUMO energy differences (the energy differences in the Rayleigh–Schrödinger perturbation expansion appears in the denominator).[45]

The group 11 metals in the oxidation state +5 may be described by the configuration $3s^23d^4$. Thus it is not clear if the spin multiplicity of the electronic ground state in CuF_6^- or even AgF_6^- corresponds to a singlet, triplet, or a quintet. We note that both CuF_6^{3-} and AgF_6^{3-} are paramagnetic in the solid state. CuF_4^- is diamagnetic. We, therefore, performed single point calculations for the triplet and quintet states of CuF_6^- and AgF_6^- at the HF, MP2, and B3LYP level of theory. For both CuF_6^- and AgF_6^- the HOMO is of t_{1u} symmetry describing an antibonding MO involving fluorine and metal *p*-orbitals. The LUMO is an antibonding e_g-orbital involving fluorine *p*- and metal *d*-orbitals. We, therefore, assume that the first triplet state has the configuration $t_{1u}^5 e_g^1$, which yields two states of *u*-symmetry, $^3T_{1u}$ and $^3T_{2u}$. Since a MC treatment to get the nondynamical electron correlation correct is beyond our computational resources, we carried out all calculations without symmetry restrictions using a spin unrestricted self-consistent field (SCF) procedure (UHF). The B3LYP minimum bond distances were chosen (1.784 Å for CuF_6^- and 1.920 Å for AgF_6^-). For CuF_6^- (AgF_6^-) we obtain the following estimates for the singlet to triplet excitation energies with respect to the $^1A_{1g}$ electronic ground state (in eV): −6.39 (−0.44) HF, 8.76 (4.93) MP2, and 0.79 (2.08) B3LYP. For the quintet excitation we obtain (in eV): −5.90 (−0.40) HF, 8.77 (8.52) MP2, and 1.68 (3.70) B3LYP. These calculations show again a large change in the excitation energy from HF to MP2. Note that in the HF

case the triplet and quintet states are lower in energy compared to the singlet state. This is understandable because exchange contributions for the $3d$-orbitals at the HF level are large and favor high spin configurations. On the other hand, electron correlation effects usually lower low-spin states more significantly. Density functional theory usually provides a balanced treatment between exchange and electron correlation and is, therefore, often superior for the treatment of transition metal compounds. Indeed, B3LYP yields only a small singlet–triplet excitation energy for CuF_6^- and predicts that CuF_6^- and AgF_6^- have ground-state singlet symmetry. The triplet and quintet states are, however, not geometry optimized and the B3LYP functional may not be very accurate for excitation energies. Both the lowest triplet and quintet states arising from the $t_{1u}^5 e_g^1$ or $t_{1u}^4 e_g^2$ configurations, respectively, would undergo a first-order Jahn–Teller distortion lowering the symmetry. To determine the correct spin symmetry for ground-state CuF_6^- requires a multiconfiguration treatment including dynamic correlation as well, a difficult task. Current single-reference methods (MP2, CISD, CCSD, etc.) are not very accurate in the case of the copper fluorides which is indicated by the large triple contributions in the coupled cluster case. We are, therefore, not able to assign the correct ground-state symmetry of CuF_6^-. We believe, however, that it is very likely that the electronic ground-state symmetry of AgF_6^- is a singlet state ($^1A_{1g}$).

The Mulliken population analyses clearly show that relativistic effects, (i) increase the valence *ns*-population, (ii) increase the $(n-1)d$ participation in *d*-orbitals which are directed towards the bonding axes, and (iii) do not change significantly the *np*-involvement which anyway is relatively small except for CuF_4^-. As expected, large relativistic changes are calculated for the fluorides of element 111 which show the highest *d*-participation of all Group 11 elements. This is due to the large relativistic $7s$ contraction and the $6d$ expansion. Another interesting feature is the relatively large $4s$ population in CuF_2^- and CuF_4^-. This is surprising since the electronegativities of Cu and Ag are quite similar (1.9 for Cu and Ag), as are the ionization potentials (7.72 eV for Cu and 7.57 eV for Ag) and electron affinities (1.23 eV for Cu and 1.30 eV for Ag).[46] Another interesting fact is that the Mulliken population analysis suggests that even the lower corelike $3s$ orbitals become slightly depopulated in CuF_6^-, a result which may, however, be an artifact of the method used.

Summarizing our results on the stability of MF_6^- compounds, the yet unknown species AgF_6^- offers the best chance for a successful synthesis, provided that bulky cations A^+ are used with a relatively small A–F bond stability in order to keep the six Ag–F bonds intact. Fluoro complexes of Group 11 metals in the oxidation state +1 are unknown. For CuF_2^- we calculated an all-electron CCSD(T) bond distance of 1.790 Å at the DK level. We mention that Zhang and Seppelt succeeded recently in isolating IF_2^- at low temperatures as 1.1.3.3.5.5-hexamethylpiperidinium difluoro iodate, $pip^+IF_2^-$.[47] AgF_2^- could be synthesized along the same routes. Disproportionation into Ag(+3) and Ag(0) is unlikely.

ACKNOWLEDGMENTS

This work was supported by European Science Foundation (REHE program), the Marsden fund Wellington (contract number 96-UOA-PSE-0081), the Auckland University Research Committee (AURC) and the High Performance Computer Committee. Comments by Professor G. A. Bowmaker and Professor P. D. W. Boyd are gratefully acknowledged. We thank Professor M. Urban and Professor B. A. Heß for the Douglas–Kroll routines.

[1] F. A. Cotton and G. Wilkinson, *Advanced Inorganic Chemistry*, 5th ed. (Wiley, New York, 1988).
[2] (a) B. Fricke, Struct. Bonding (Berlin) **21**, 89 (1975); (b) For a recent review on the chemistry of transactinides see: V. Pershina, Chem. Rev. **96**, 1977 (1996).
[3] S. Hofmann, V. Ninov, F. P. Heßberger, P. Armbruster, H. Folger, G. Münzenberger, H. J. Schött, A. G. Popeko, A. V. Yeremin, A. N. Andreyev, S. Saro, R. Janik, and M. Leino, Z. Phys. A **350**, 281 (1995).
[4] (a) D. C. Hoffman, Chem. Eng. News **72**, 24 (1994); (b) D. C. Hoffman, Radiochim. Acta **61**, 123 (1993); (c) M. Schädel, *ibid.* **70/71**, 207 (1995).
[5] G. Herrmann, Angew. Chem. Int. Ed. Engl. **34**, 1713 (1995).
[6] (a) G. L. Gutsev and A. I. Boldyrev, Mol. Phys. **53**, 23 (1984); (b) G. L. Gutsev and A. I. Boldyrev, Russ. J. Inorg. Chem. **34**, 169 (1989); (c) A. E. Dorigo, J. Wanner, and P. v. R. Schleyer, Angew. Chem. Int. Ed. Engl. **34**, 476 (1995).
[7] P. Schwerdtfeger, J. Am. Chem. Soc. **111**, 7261 (1989).
[8] P. Schwerdtfeger, P. D. W. Boyd, S. Brienne, and A. K. Burrell, Inorg. Chem. **31**, 3411 (1992).
[9] P. Pyykkö, Chem. Rev. **88**, 563 (1988).
[10] W. H. E. Schwarz, *Fundamentals of Relativistic Effects in Chemistry*, in *Theoretical Models of Chemical Bonding, Vol. II*, edited by Z. B. Maksic (Springer, Heidelberg, 1989), p. 593.
[11] B. A. Heß, Ber. Bunsenges. Phys. Chem. **101**, 1 (1997).
[12] P. Schwerdtfeger, M. Dolg, W. H. E. Schwarz, G. A. Bowmaker, and P. D. W. Boyd, J. Chem. Phys. **91**, 1762 (1989).
[13] (a) P. Schwerdtfeger, P. D. W. Boyd, A. K. Burrell, and M. J. Taylor, Inorg. Chem. **29**, 3593 (1990); (b) P. Pyykkö and Y. Zhao, Chem. Phys. Lett. **177**, 103 (1991); (c) P. Schwerdtfeger and M. Dolg, Phys. Rev. A **43**, 1644 (1991); (d) P. Schwerdtfeger and G. A. Bowmaker, J. Chem. Phys. **100**, 4487 (1994); (e) L. Antes, S. Dapprich, G. Frenking, and P. Schwerdtfeger, Inorg. Chem. **35**, 2089 (1996).
[14] E. Eliav, U. Kaldor, P. Schwerdtfeger, B. A. Hess, and Y. Ishikawa, Phys. Rev. Lett. **73**, 3203 (1994).
[15] M. Seth, M. Dolg, K. Faegri, B. A. Heß, U. Kaldor, and P. Schwerdtfeger, Chem. Phys. Lett. **250**, 461 (1996).
[16] T. Fleischer and R. Hoppe, Z. Anorg. Allg. Chem. **492**, 76 (1982).
[17] R. Hoppe, Z. Anorg. Allg. Chem. **292**, 28 (1957).
[18] (a) A. G. Sharpe, J. Chem. Soc. **1950**, 3444; (b) R. Hoppe and W. Z. Klemm, Z. Anorg. Allg. Chem. **268**, 364 (1952).
[19] K. Leary and N. Bartlett, J. Chem. Soc. Chem. Commun. **1972**, 903.
[20] A. J. Edwards, J. Chem. Soc. A **1969**, 1936.
[21] (a) K. Leary, A. Zalkin, and N. Bartlett, J. Chem. Soc. Chem. Commun. **1973**, 131; (b) K. Leary, A. Zalkin, and N. Bartlett, Inorg. Chem. **13**, 775 (1974).
[22] M. Dolg, U. Wedig, H. Stoll, and H. Preuss, J. Chem. Phys. **86**, 866 (1987).
[23] D. Andrae, U. Häussermann, M. Dolg, and H. Stoll, Theor. Chim. Acta **77**, 123 (1990).
[24] D. Andrae, Ph.D. thesis, University of Stuttgart, Stuttgart (1989).
[25] M. Seth, P. Schwerdtfeger, and M. Dolg, J. Chem. Phys. **106**, 3623 (1997).
[26] ATMSCF, R. M. Pitzer (Ohio State University, Columbus, 1979).
[27] (a) S. R. Langhoff and C. W. Bauschlicher, Chem. Phys. Lett. **124**, 241 (1986); (b) R. L. Martin, J. Chem. Phys. **86**, 5027 (1987); (c) P. Schwerdtfeger, Chem. Phys. Lett. **183**, 457 (1991).
[28] (a) T. H. Dunning, J. Chem. Phys. **90**, 1007 (1989); (b) R. A. Kendall, T. H. Dunning, and R. J. Harrison, *ibid.* **96**, 6796 (1992).
[29] GAUSSIAN94, Rev. D.1, M. J. Frisch, G. W. Trucks, H. B. Schlegel, P. M. W. Gill, B. G. Johnson, M. A. Robb, J. R. Cheeseman, T. Keith, G. A. Petersson, J. A. Montgomery, K. Raghavachari, M. A. Al-Laham, V. G. Zakrzewski, J. V. Ortiz, J. B. Foresman, J. Cioslowski, B. B. Stefanov, A.

Nanayakkara, M. Challacombe, C. Y. Peng, P. Y. Ayala, W. Chen, M. W. Wong, J. L. Andres, E. S. Replogle, R. Gomperts, R. L. Martin, D. J. Fox, J. S. Binkley, D. J. DeFrees, J. Baker, J. J. P. Stewart, M. Head-Gordon, C. Gonzalez, and J. A. Pople (Gaussian, Inc., Pittsburgh, PA, 1996).
[30] MOLCAS 3, K. Andersson, M. P. Fülscher, G. Karlström, R. Lindh, P-Å Malmqvist, J. Olsen, B. O. Roos, A. J. Sadlej, M. R. A. Blomberg, P. E. M. Siegbahn, V. Kellö, J. Noga, M. Urban, and P-O. Widmark (Lund, Sweden, 1994).
[31] M. Pelissier, N. Komiha, and J. P. Daudey, J. Comput. Chem. **9**, 298 (1988).
[32] TITAN, T. J. Lee, J. E. Rice, and A. P. Rendell (NASA Ames Research Center, Moffet Field, California, 1990).
[33] K. Raghavachari and G. W. Trucks, J. Chem. Phys. **91**, 1062 (1989).
[34] P. Schwerdtfeger and J. Ischtwan, J. Mol. Struct.: THEOCHEM **306**, 9 (1994).
[35] H. Partridge, J. Chem. Phys. **90**, 1043 (1989).
[36] C. W. Bauschlicher, Theor. Chim. Acta **92**, 183 (1995).
[37] M. Douglas and N. M. Kroll, Ann. Phys. (Leipzig) **82**, 89 (1974).
[38] (a) B. A. Heß, Phys. Rev. A **39**, 3742 (1986); (b) R. Samzov, B. A. Heß, and G. Jansen, J. Chem. Phys. **96**, 1227 (1992).
[39] P. Schwerdtfeger (unpublished results).
[40] M. A. Buijse and E. J. Baerends, J. Chem. Phys. **93**, 4129 (1990).
[41] C. Lee, W. Yang, and R. G. Parr, Phys. Rev. B **37**, 785 (1988).
[42] (a) A. D. Becke, Phys. Rev. A **38**, 3098 (1988); (b) A. D. Becke, J. Chem. Phys. **98**, 5648 (1993).
[43] (a) COLUMBUS, R. Shepard, I. Shavitt, R. M. Pitzer, D. C. Comeau, M. Pepper, H. Lischka, P. G. Szalay, R. Ahlrichs, F. B. Brown, and J. G. Zhao, Int. J. Quantum Chem., Symp. **22**, 149 (1989); (b) A. Chang and R. M. Pitzer, J. Am. Chem. Soc. **111**, 2500 (1989); (c) A. Chang and R. M. Pitzer, ARGOS, CNVRT, SCFPQ, LSTRN, and spin–orbit CI program.
[44] K. P. Huber and G. Herzberg, *Molecular Spectra and Molecular Structure Constants of Diatomic Molecules* (Van Nostrand, New York, 1979).
[45] P. M. W. Gill, M. W. Wong, R. H. Nobes, and L. Radom, Chem. Phys. Lett. **148**, 541 (1988).
[46] (a) C. E. Moore, Atomic Energy Levels, Natl. Bur. Stand. Circ. No. 467, U.S. Government Printing Office, Washington, D.C. (1958); (b) H. Hotop and W. C. Lineberger, J. Phys. Chem. Ref. Data **14**, 731 (1985).
[47] X. Zhang and K. Z. Seppelt, Z. Anorg. Allg. Chem. **623**, 491 (1997).